10.48047/jocaaa.2024.33.07.56

Computational Analysis and Experimental Evaluation of Novel Pyrrole–Pyrimidine Carboxylates as Potential Antidiabetic Agents

Rashmi S Chouthe[a,b], Rahul P. Kshirsagar [c], Jaiprakash N. Sangshetti[a], Manoj G Damale[b], Hemant D Une [a]*.

[a] Y. B. Chavan College of Pharmacy, Chhatrapati Sambhajinagar (Aurangabad) Maharashtra, India – 431001.
[b]Srinath College of Pharmacy, Bajaj Nagar Waluj, Chhatrapati Sambhajinagar (Aurangabad) 431136, India
[c]Shri Chhatrapati Shivaji College of Pharmacy, Kannad, Chhatrapati Sambhajinagar (Aurangabad) 431103, India

*Correspondence to:
Prof. Dr Hemant D Une
Professor, Y. B. Chavan College of Pharmacy, Chhatrapati Sambhajinagar (Aurangabad)
Maharashtra, India – 431001.
Office: +91-0240-2391752 /2381129
Fax: +91-0240-2391752 /2381129
E-mail: hemantdune@gmail.com

ABSTRACT

Diabetes mellitus remains a major global health challenge and is strongly linked to metabolic disturbances including obesity, hypertension, cardiovascular complications, and atherosclerosis. In the present study, a series of novel pyrrole–pyrimidine carboxylate derivatives were designed and synthesized using an efficient one-pot multicomponent reaction strategy. Structural confirmation of the synthesized hybrids was achieved through thin-layer chromatography, melting point analysis, and spectroscopic characterization. To explore their therapeutic relevance, a comprehensive computational investigation was performed, focusing on molecular docking interactions with the insulin receptor. Docking studies, carried out using AutoDock Tools 1.5.4, revealed strong binding affinities for several derivatives, particularly compounds **4h, 4g, 4i, and 4d**, indicating their potential as promising antidiabetic scaffolds.

To support the in silico findings, selected compounds were further assessed in vivo using a nicotinamide–streptozotocin (NA–STZ) induced type II diabetic rat model. Consistent with the computational predictions, compound **4h (30 mg/kg)** produced a marked reduction in fasting blood glucose levels, while **4g (30 mg/kg)** exhibited a moderate but significant effect. Both compounds also attenuated oxidative stress by lowering lipid peroxidation (MDA) and enhancing antioxidant defenses such as superoxide dismutase (SOD) and glutathione (GSH) in hepatic and pancreatic tissues.

10.48047/jocaaa.2024.33.07.56

Overall, the integrated computational and biological evaluation underscores the potential of pyrrole–pyrimidine carboxylate derivatives—especially 4h and 4g—as promising leads for developing effective antidiabetic agents.

KEYWORDS:

Molecular docking, Pyrrole derivative, Antidiabetic, In silico evaluation, Streptozotocin (STZ) and Nicotinamide (NA) model.

1. INTRODUCTION

Diabetes mellitus is a major global health concern, affecting 537 million adults in 2021, with projections rising to 783 million by 2045 [1,2]. It is characterized by chronic hyperglycemia due to impaired insulin secretion or action, leading to complications such as cardiovascular disease, nephropathy, retinopathy, and neuropathy [3,4]. The worldwide economic burden exceeds $966 billion annually, emphasizing the need for new therapeutic options [5,6].

Current treatments aim to regulate blood glucose by improving insulin sensitivity, enhancing insulin secretion, reducing glucose absorption, or suppressing glucose production [7,8]. However, these therapies often cause hypoglycemia, weight gain, gastrointestinal side effects, and reduced long-term efficacy, driving the search for safer and more effective agents [9,10]. Nitrogen-based heterocycles, particularly pyrrole and pyrimidine, have gained importance due to their structural similarity to biomolecules and wide pharmacological activity [11–14]. Pyrrole is present in key biological compounds such as heme and chlorophyll [15,16], while pyrimidine forms the core of nucleic acids and exhibits diverse medicinal properties [17,18].

Combining pyrrole and pyrimidine in a single scaffold has shown promising results in developing antidiabetic molecules, offering improved activity, selectivity, and reduced toxicity [19–22]. Pyrrole derivatives demonstrate antidiabetic potential through α-glucosidase, DPP-4, and PTP1B inhibition, as well as insulin receptor activation [23–25]. Additionally, pyrrolidine-based small molecules are emerging as versatile antidiabetic and anticancer agents.

10.48047/jocaaa.2024.33.07.56

Carboxylate groups serve as important pharmacophores, enhancing molecular recognition, binding, and bioavailability [26,27]. Their incorporation into heterocycles has contributed to successful drugs, including metformin and phenformin [28,29]. Through hydrogen bonding and electrostatic interactions, carboxylate moieties significantly influence pharmacokinetic and pharmacodynamic profiles (Figure 1) [30,31].

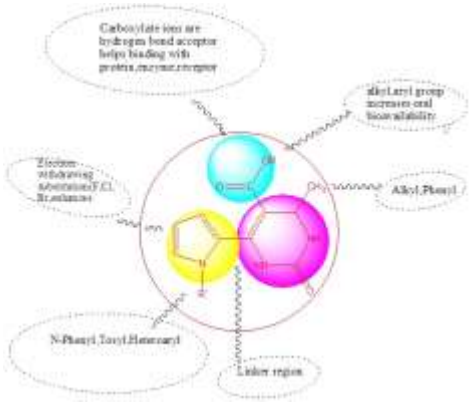

Figure 1 Structural Feature of designed Pyrrole-pyrimidine carboxylate compound

SAR investigations show that substituent orientation on pyrrole–pyrimidine scaffolds strongly affects antidiabetic activity [32,33]. Carboxylate groups, due to their electron-withdrawing nature, enhance target interactions and improve solubility and permeability, making them valuable in drug design [34–37].

α-Glucosidase inhibition remains an established strategy for controlling postprandial hyperglycemia, as the enzyme mediates the final step of carbohydrate digestion [38–41]. Its inhibition delays glucose absorption and stabilizes postprandial glucose levels [42,43]. However, existing inhibitors like acarbose and miglitol cause gastrointestinal discomfort, encouraging the search for safer agents [44,45].PTP1B is another key antidiabetic target due to its negative regulation of insulin signaling [46–49]. Selective inhibitors of this enzyme show potential for improving insulin sensitivity and glucose control [50,51].

Advances in computational drug design—especially molecular docking and QSAR—now play a central role in identifying and optimizing bioactive compounds by predicting ligand–target interactions efficiently and cost-effectively [52–57].Both pyrimidine-based drugs such

10.48047/jocaaa.2024.33.07.56

as pioglitazone [58,59] and pyrrole derivatives with α-glucosidase inhibitory activity [60,61] highlight the relevance of these scaffolds. Designing effective antidiabetic agents requires addressing target selectivity, metabolic stability, and safety [62,63]. Hybrid molecules combining pyrrole, pyrimidine, and carboxylate units offer a promising strategy for achieving higher potency and fewer side effects [64–67].

Given the need for improved antidiabetic therapies, pyrrole-pyrimidine carboxylates provide a rational platform for new drug development [68,69]. This study focuses on designing and synthesizing such hybrids and evaluating their antidiabetic potential through molecular docking and in vivo testing in the STZ–NA rat model to identify promising lead candidates [70,71].

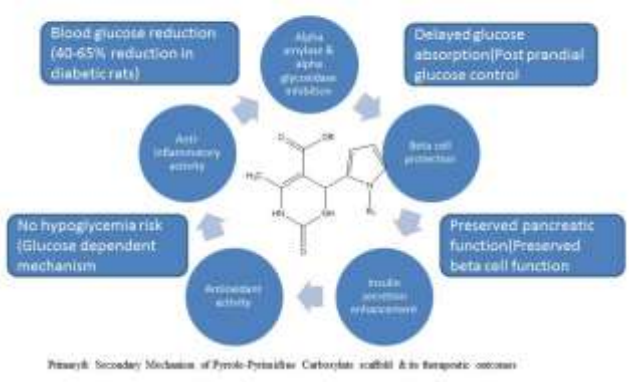

Figure 2 - Primary & Secondary Mechanism of Pyrrole-pyrimidine carboxylate scaffold & its therapeutic outcome

2. EXPERIMENTAL

Laboratory-grade reagents required for synthesizing pyrrole–pyrazine carboxylate derivatives were procured from SD Fine Chemicals Pvt. Ltd. (Mumbai), TCI Pvt. Ltd. (Chennai), Fisher Scientific (Mumbai), and Avra Synthesis Pvt. Ltd. (Hyderabad). Streptozotocin and nicotinamide were obtained from Sisco Research Laboratories Pvt. Ltd. (Taloja, India). All chemicals were used as received without further purification. AutoDock

10.48047/jocaaa.2024.33.07.56

Tools 1.5.4 (ADT) was used to generate input files for docking studies [72]. Melting points were recorded using a digital melting point apparatus. FTIR spectra were used for primary functional group identification. ^{1}H and ^{13}C NMR spectra were acquired on a Bruker 500 MHz spectrometer at SAIF, Punjab. Mass spectra were obtained using a Shimadzu GC–MS QP 5000 system. Reaction progress and product purity were monitored by TLC on silica gel F254 plates (E. Merck, Germany) using methanol, ethyl acetate, and n-hexane as mobile phases, with spots visualized under iodine vapors.

2.1 Procedure for synthesis of Pyrrole-pyrimidine carboxylate derivatives

The alkyl substituted 1,2,3,4-tetrahydro-6-methyl-2-oxo-4-(1H-pyrrol-2-yl)pyrimidine-5-carboxylate (4a-4e) and 1,2,3,4-tetrahydro-6-methyl-2-oxo-4-(1-tosyl-1H-pyrrol-2-yl)pyrimidine-5-carboxylate (4f-4j) derivatives were synthesized as summarized in (Scheme 1) 4(a–j) were synthesized by reacting a mixture of 1H- pyrrole 2 carbaldehyde ,1tosyl 1H-pyrrole 2 carbaldehyde(1/1') alkyl substituted ester (2a-j) , urea (3) , Oxalic acid (10 mol%) as a catalyst, all the reactants was dissolved in ethanol (20 ml) and this mixture was irradiated in microwave synthesizer for 15 to 20 min at 225w till completion of reaction indicated on TLC.

The reaction mixture was cooled to room temperature and poured on ice-water (50 ml) to get the precipitated solid. It was collected by filtration, washed with water and dried to give the corresponding tetra substituted pyrrole-pyrimidine carboxylate derivatives. All the synthesized compounds were characterized and confirmed by spectral analysis like; FTIR, 1H-NMR, 13C-NMR, MS. The purity of the synthesized compounds was determined by thin layer chromatography (TLC). The melting points were determined in open capillary tubes by using digital melting point apparatus and are uncorrected. Physical constants data and the time required for completion of reactions for the alkyl substituted 1,2,3,4-tetrahydro-6-methyl-2-oxo-4-(1H-pyrrol-2-yl)pyrimidine-5-carboxylate (4a-4e) and 1,2,3,4-tetrahydro-6-methyl-2-oxo-4-(1-tosyl-1H-pyrrol-2-yl)pyrimidine-5-carboxylate (4f-4j) derivatives are summarized in Table 1

10.48047/jocaaa.2024.33.07.56

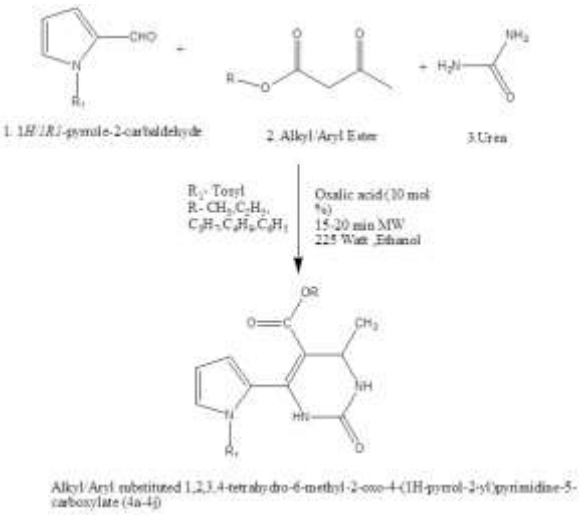

Scheme 1- Synthesis of Designed Pyrrole-Pyrimidine Carboxylate by one pot multicomponent approach

Table 1 Physical constants data and the time required for completion of reactions for the alky substituted 1,2,3,4-tetrahydro-6-methyl-2-oxo-4-(1H-pyrrol-2-yl)pyrimidine-5-carboxylate 4(a–j)

Sr No	Derivative	Ester	Molecular formula	Molecular weight	Time (225W, 75-80 °C)	Yield	M. P
1	4a	Methyl acetoacetate	$C_{11}H_{13}N_3O_3$	235	17min	78 %	272
2	4b	Ethyl acetoacetate	$C_{12}H_{15}N_3O_3$	249	15min	80%	278
3	4c	Propyl acetoacetate	$C_{13}H_{17}N_3O_3$	263	18min	60 %	292
4	4d	Butyl acetoacetate	$C_{14}H_{19}N_3O_3$	277	18min	80%	282
5	4e	Phenyl acetoacetate	$C_{16}H_{15}N_3O_3$	297	15min	73%	298
6	4f	Methyl acetoacetate	$C_{18}H_{19}N_3O_5S$	389.5	18min	55%	270
7	4g	Ethyl acetoacetate	$C_{19}H_{21}N_3O_5S$	403.5	16min	65%	284
8	4h	Propyl acetoacetate	$C_{20}H_{23}N_3O_5S$	417.5	15min	60 %	258
9	4i	Butyl acetoacetate	$C_{21}H_{25}N_3O_5S$	431.5	17min	75%	288
10	4j	Phenyl acetoacetate	$C_{23}H_{21}N_3O_5S$	451.5	16min	78%	296

Commented [1]: Temperature is not mentioned in table

2.2 Molecular Docking studies

10.48047/jocaaa.2024.33.07.56

Auto Dock Tools 1.5.4 (ADT) was used to generate ligand and receptor input files for molecular docking [72]. Before docking, crystallographic protein structures were prepared by removing water molecules and ions. Polar hydrogens were added, and Kollman united atom charges were assigned [73–74]. Residue pKa values were predicted using PROPKA 2.0 to ensure correct protonation states [75]. Accordingly, lysine, arginine, and histidine residues were protonated, while glutamic and aspartic acids were kept deprotonated.Ligand preparation involved merging nonpolar hydrogens, assigning Gasteiger charges, defining rotatable bonds, and saving structures in pdbqt format. A grid box of 40 × 40 × 40 Å (1 Å) was positioned around the enzyme's active site, centered on the coordinates of the co-crystallized ligand. All other AutoDock Vina parameters were maintained at default settings.

2.3 Experimental Animals

Male Wistar rats (180–220 g) and female Swiss albino mice (25–30 g) were sourced from Cape Bio Lab & Research Centre, Marthandam, India. Animals were acclimatized for one week under controlled conditions (23 ± 2 °C, 55 ± 5% RH, 12-h light/dark cycle) with free access to standard feed and water. All procedures were approved by the Institutional Animal Ethics Committee in accordance with CPCSEA guidelines (Protocol No. CBLRC/IAE/01/02-2022).

2.4 Acute Toxicity Studies

Acute oral toxicity was evaluated in female Swiss albino mice following OECD Guideline 423 [86]. Mice (n = 3 per group) were fasted overnight and administered hybrids 4h or 4g at 300 mg/kg suspended in 0.5% CMC. Animals were observed for clinical signs during the first 24 h and daily thereafter for 21 days.

2.5 In Vivo Antidiabetic Activity

2.5.1 Induction of Diabetes

Type 2 diabetes was induced using nicotinamide (110 mg/kg, i.p.) followed after 30 min by streptozotocin (60 mg/kg, i.p.) in citrate buffer (pH 4.5). A 5% glucose solution was given for 24 h to prevent hypoglycemia [88]. Fasting blood glucose (FBG) was measured after 72 h; rats with FBG > 180 mg/dL were included as diabetic, while normal controls had FBG < 100 mg/dL.

2.5.2 Experimental Design

10.48047/jocaaa.2024.33.07.56

Rats (n = 42) were allocated into seven groups (n = 6). After overnight fasting, baseline body weight and FBG were recorded. Diabetic groups received metformin (100 mg/kg) or test compounds 4f and 4b at 15 or 30 mg/kg. All treatments were administered orally in 0.5% CMC twice daily for 21 days [89]. FBG and body weight were monitored on Days 0, 1, 7, 15, and 21. Dose selection was based on preliminary studies and reported activity of similar pyrrole derivatives [90].Statistical analysis was performed in GraphPad Prism 9.0 using ANOVA with Tukey's post hoc test or Kruskal–Wallis with Dunn's test, as appropriate. Significance was set at $p < 0.05$.

2.5.3 Collection of Blood and Tissue Samples

On Day 21, blood was collected from the carotid artery. Serum and plasma were separated and stored at –80 °C. Animals were euthanized by CO_2 inhalation and pancreas and liver tissues were fixed in 10% formalin.

2.5.4 Plasma Glucose, Insulin, and Lipid Profile

Plasma glucose, TG, TC, LDL, and HDL were estimated using commercial diagnostic kits (Bio-Systems, Spain) on a semi-automated analyzer. Insulin levels were measured by RIA (CisBio). HOMA-IR was calculated as: **HOMA-IR = (fasting glucose × fasting insulin) / 405**

2.6 Oxidative Stress Markers

2.6.1 Malondialdehyde (MDA)

Lipid peroxidation was quantified using the TBA method [91]. Tissue homogenate was reacted with TCA and TBA, heated at 90 °C, cooled, and absorbance was recorded at 532 nm. Results were expressed as nM/g tissue.

2.6.2 Superoxide Dismutase (SOD)

SOD activity was assessed by inhibition of pyrogallol autoxidation [92,93]. Absorbance change at 420 nm was monitored for 2 min, and activity was reported as U/g tissue.

2.6.3 Reduced Glutathione (GSH)

10.48047/jocaaa.2024.33.07.56

GSH content was measured by reaction with DTNB after protein precipitation with TCA. Absorbance was read at 412 nm, and results were expressed as μM/g tissue [94,95].

3. RESULTS & DISCUSSION

The present investigation demonstrates the successful design, synthesis, and biological evaluation of novel pyrrole-pyrimidine carboxylate derivatives as potential antidiabetic agents. The comprehensive approach employed in this study, encompassing computational molecular docking, efficient synthetic methodology, and rigorous biological assessment, has yielded significant insights into the structure-activity relationships and therapeutic potential of these compounds.

3.1Chemistry

The microwave-assisted one-pot multicomponent method enabled rapid and efficient synthesis of pyrrole-pyrimidine carboxylate derivatives, completing reactions within 15–20 minutes compared to several hours by conventional heating. This approach improved yields, minimized by-products, and adhered to green chemistry by reducing solvent use, energy consumption, and waste. Uniform microwave heating also ensured reproducibility and high product purity.

The method generated a diverse library of derivatives, confirmed by spectroscopic analysis. SAR studies showed that electron-withdrawing groups (F, Cl) at the 3-position of the pyrrole ring enhanced α-amylase and α-glucosidase inhibition. Ethyl carboxylate derivatives (4b, 4g) were more active than methyl analogs, likely due to stronger hydrophobic interactions, while branched groups reduced activity due to steric effects. Substitution at the pyrimidine 2-position with small alkyl groups (methyl/ethyl) favored potency, whereas bulkier substituents decreased activity.

10.48047/jocaaa.2024.33.07.56

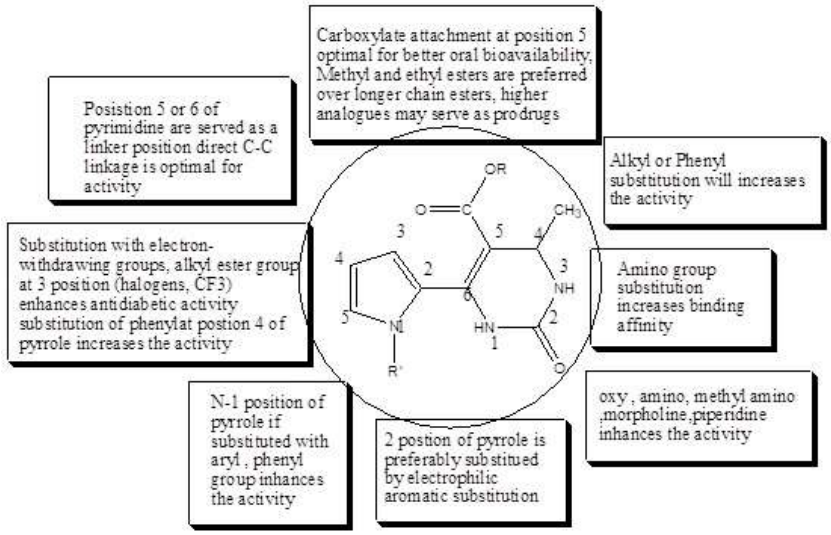

Figure3 SAR analysis of Pyrrole-pyrimidine carboxylate analogues revealed several critical structural features essential for optimal biological activity

Spectral Data

Methyl 1,2,3,4-tetrahydro-4-methyl-2-oxo-6-(1H-pyrrol-2-yl)pyrimidine-5-carboxylate(4a) obtain as yellow colour solid in 78% yield , M P 272 -273°C ^{1}HNMR (Bruker 500MHz, CDCl3) 6.1 CH –Pyrrole,6.32 CH –Pyrrole,6.62 CH –Pyrrole,5.1-NH –Pyrrole, 6.48 NH –pyrimidine,6 .48 NH –pyrimidine,4.45 CH –methine,1.40 CH_3 –Methyl,3.76-CH_3 –Methyl,^{13}CNMR 108.6, 118,118.3,111, 140.9,150.4,23.9,110.4,167.2,18.8, 52.3 Mass spectrum E/Z $[M+H]^+$-$C_{11}H_{13}N_3O_3$Calculated - 235, found – 235.567.

Ethyl 1,2,3,4-tetrahydro-4-methyl-2-oxo-6-(1H-pyrrol-2-yl)pyrimidine-5-carboxylate (4b) obtain as yellow colour solid in 80% yield , M P 278 -280°C ^{1}HNMR (Bruker 500MHz, CDCl3) 6.1 CH –Pyrrole,6.32 CH –Pyrrole,6.62 CH –Pyrrole,5.1-NH –Pyrrole, 6.48 NH –pyrimidine,6 .48 NH –pyrimidine,4.45 CH –methine,1.40 CH_3 –Methyl, 4.19 –CH_2 3.76-CH_3 –Methyl,^{13}CNMR 108.6, 118,118.3,111, 143,150.4,23.9,108,167.2,18.8, 14.3 61.4 Mass spectrum E/Z $[M+H]^+$-$C_{12}H_{15}N_3O_3$Calculated - 249, found – 250.314.

Propyl 1,2,3,4-tetrahydro-4-methyl-2-oxo-6-(1H-pyrrol-2-yl)pyrimidine-5-carboxylate (4c) obtain as pale yellow colour solid in 60% yield , M P 292 -293°C ^{1}HNMR (Bruker 500MHz, CDCl3) 6.3 CH –Pyrrole,6.4 CH –Pyrrole,6.62 CH –Pyrrole,5.1-NH –Pyrrole, 6.48 NH –

10.48047/jocaaa.2024.33.07.56

pyrimidine,6 .48 NH –pyrimidine,4.45 CH –methine,1.40 CH_3 –Methyl, 4.19 –CH_2 3.76-CH_3 Methyl, 1.01 CH_3–Methyl,^{13}CNMR 108.6, 118,118.3,111,143,150.4,23.9,108,167.2,18.8, 12.3,10.3, 67.4 Mass spectrum E/Z $[M+H]^+$-$C_{13}H_{17}N_3O_3$Calculated - 263, found – 263.814.

Butyl 1,2,3,4-tetrahydro-4-methyl-2-oxo-6-(1H-pyrrol-2-yl)pyrimidine-5-carboxylate (4d)obtain as pale yellow colour solid in 60% yield , M P 292 -293°C ^{1}HNMR (Bruker 500MHz, CDCl3) 6.3 CH –Pyrrole,6.4 CH –Pyrrole,6.62 CH –Pyrrole,5.1-NH –Pyrrole, 6.48 NH –pyrimidine,6 .48 NH –pyrimidine,4.45 CH –methine,1.40 CH_3 –Methyl, 4.19 –CH_2 3.76-CH_3 Methyl, 1.01 CH_3–Methyl,^{13}CNMR 108.6, 118,118.3,111,143,150.4,23.9,108,167.2,18.8, 12.3,10.3, 67.4 Mass spectrum E/Z $[M+H]^+$-$C_{13}H_{17}N_3O_3$Calculated - 263, found – 263.814.

Phenyl 1,2,3,4-tetrahydro-4-methyl-2-oxo-6-(1H-pyrrol-2-yl)pyrimidine-5-carboxylate (4e) obtain as yellow colour solid in 73% yield , M P 298 -299°C ^{1}HNMR (Bruker 500MHz, CDCl3) 6.3 CH –Pyrrole,6.4 CH –Pyrrole,6.62 CH –Pyrrole,5.1-NH –Pyrrole, 6.48 NH –pyrimidine,6 .48 NH –pyrimidine,4.45 CH –methine,1.40 CH_3 –Methyl, 7.40 –CH-Benzene 7.76-CH Benzene 7.01 CH Benzene, 7.96 CH Benzene ,7.10- CH Benzene ^{13}CNMR 108.6, 118,118.3,111,143,150.4,23.9,108,167.2,121.3,129.2,151.4,121,129.4,125.4 Mass spectrum E/Z $[M+H]^+$-$C_{16}H_{15}N_3O_3$Calculated - 297, found – 298.321.

Methyl-1,2,3,4-tetrahydro-6-methyl-2-oxo-4-(1-tosyl-1H-pyrrol-2-yl)pyrimidine-5-carboxylate (4f) obtain as yellow colour solid in 55% yield , M P 270-272°C ^{1}HNMR (Bruker 500MHz, CDCl3) 6.1 NH-Pyridine, 5.56-CH-methine, 6.0-NH-Pyridine, 5.7,5.9,6.4- CH-Pyrrole, 7.81 CH-Benzene, 7.31 CH-Benzene, 2.35- CH3,7.34,7.81- CH –Benzene,1.71 CH_3-Methyl,3.76 OCH_3 ^{13}CNMR150.3,42.2,108.9,145.3,167,131.1,106.8,108.2,121.1,134.2,128.2,130.9,143.2,24.2,130.1128.2,14.1,52.3 Mass spectrum E/Z $[M+H]^+$-$C_{18}H_{19}N_3O_5S$ Calculated - 389.5, found – 390.321.

Ethyl-1,2,3,4-tetrahydro-6-methyl-2-oxo-4-(1-tosyl-1H-pyrrol-2-yl)pyrimidine-5-carboxylate (4g) obtain as yellow colour solid in 65% yield , M P 284-286°C ^{1}HNMR (Bruker 500MHz, CDCl3) 6.1 NH-Pyridine, 5.56-CH-methine, 6.0-NH-Pyridine, 5.7,5.9,6.4- CH-Pyrrole, 7.81 CH-Benzene, 7.31 CH-Benzene, 2.35- CH3,7.34,7.81- CH –Benzene,1.71 CH_3-Methyl,3.76 CH_2,1.30-CH_3 ^{13}CNMR150.3,42.2,108.9,145.3,167,131.1,106.8,108.2,121.1,134.2,128.2,130.9,143.2,24.2,130.1128.2,14.1,52.3 ,14.2 Mass spectrum E/Z $[M+H]^+$-$C_{19}H_{21}N_3O_5S$ Calculated - 403, found – 403.629.

10.48047/jocaaa.2024.33.07.56

Propyl-1,2,3,4-tetrahydro-6-methyl-2-oxo-4-(1-tosyl-1H-pyrrol-2-yl)pyrimidine-5-carboxylate (4h) obtain as yellow colour solid in 65% yield , M P 284-286°C ^{1}HNMR (Bruker 500MHz, CDCl3) 6.1 NH-Pyridine, 5.56-CH-methine, 6.0-NH-Pyridine, 5.7,5.9,6.4- CH-Pyrrole, 7.81 CH-Benzene, 7.31 CH-Benzene, 2.35- CH3,7.34,7.81- CH –Benzene,1.71 CH_3-Methyl,3.76 CH_2,1.30-CH_3,0.96-CH3Methyl ^{113}CNMR150.3,42.2,108.9,145.3,167,131.1,106.8,108.2,121.1,134.2,128.2,130.9,143.2,24.2,130.1128.2,14.1,52.3 ,14.2,10.3 Mass spectrum E/Z $[M+H]^+$-$C_{20}H_{23}N_3O_5S$ Calculated - 417, found – 418.221.

Butyl-1,2,3,4-tetrahydro-6-methyl-2-oxo-4-(1-tosyl-1H-pyrrol-2-yl)pyrimidine-5-carboxylate (4i) obtain as yellow colour solid in 75% yield , M P 288-289°C ^{1}HNMR (Bruker 500MHz, CDCl3) 6.1 NH-Pyridine, 5.56-CH-methine, 6.0-NH-Pyridine, 5.7,5.9,6.4- CH-Pyrrole, 7.81 CH-Benzene, 7.31 CH-Benzene, 2.35- CH3,7.34,7.81- CH –Benzene,1.71 CH_3-Methyl,3.76 CH_2,1.30-CH_3,0.96-CH3Methyl ^{113}CNMR150.3,42.2,108.9,145.3,167,131.1,106.8,108.2,121.1,134.2,128.2,130.9,143.2,24.2,130.1128.2,14.1,52.3 ,14.2,19.3,13.8 Mass spectrum E/Z $[M+H]^+$-$C_{21}H_{25}N_3O_5S$ Calculated - 431, found – 432.121.

Phenyl-1,2,3,4-tetrahydro-6-methyl-2-oxo-4-(1-tosyl-1H-pyrrol-2-yl)pyrimidine-5-carboxylate (4j) obtain as yellow colour solid in 78% yield , M P 296-298°C ^{1}HNMR (Bruker 500MHz, CDCl3) 6.1 NH-Pyridine, 5.56-CH-methine, 6.0-NH-Pyridine, 5.7,5.9,6.4- CH-Pyrrole, 7.81 CH-Benzene, 7.31 CH-Benzene, 2.35- CH3,7.34,7.81- CH –Benzene,1.71 CH_3-Methyl,3.76 CH_2,7.30-CH.Benzene, 7.33-CH.Benzene 7.96-CH-Benzene, 7.01 CH-Benzene,7.33-CH-Benzene ^{113}CNMR150.3,42.2,108.9,145.3,167,131.1,106.8,108.2,121.1,134.2,128.2,130.9,143.2,24.2,130.128.2,14.1,151.1,121.3,124.3,121.2,129.2,129.8 Mass spectrum E/Z $[M+H]^+$-$C_{20}H_{23}N_3O_5S$ Calculated - 451.5, found – 452.785

3.2 In silico studies

3.2.1Molecular Docking

Dipeptidyl peptidase-IV (DPP-IV) is a key serine protease involved in glucose regulation and is a well-established target for type 2 diabetes therapy. It degrades incretin hormones (GLP-1

10.48047/jocaaa.2024.33.07.56

and GIP), which normally enhance insulin release and suppress glucagon. Inhibiting DPP-IV increases incretin levels and improves glycemic control.

Molecular docking of the synthesized derivatives was performed against DPP-IV to assess binding energy, affinity, and interactions. The X-ray crystal structure of human DPP-IV complexed with a cyclohexylamine inhibitor (PDB: 2P8S, 2.20 Å) was used [76–78]. Redocking of the co-crystallized ligand was carried out to validate the docking protocol, and the active site was defined based on crystallographic data.

Compound ID	**Docking Score(pdb id 2P8S) [Kcal/Mol]**	**RMSD Å**
4a	-4.3104	0.15
4b	-4.1925	0.11
4c	-4.7670	0.14
4d	-4.7336	0.11
4e	-4.5107	0.10
4f	-4.2107	0.14
4g	-5.5231	0.13
4h	-5.7655	0.10
4i	-5. 4630	0.17
4j	-3.6285	0.13
417(Co crystallized ligand)	-5.6371	0.11

Table 2 Molecular docking details of synthesized Pyrrole-pyrimidine carboxylate derivatives

The most active derivative, **4h** (−5.76 kcal/mol), showed key interactions within the DPP-IV active site. The sulfonyl group formed conventional H-bonds with **ARG125** and **SER630** (2.72 and 2.02 Å). **ASP206** interacted with the dihydropyrimidinone –NH (2.15 Å), while **TYR662** formed an additional H-bond (2.28 Å). **TYR547** exhibited π–lone pair, π–π stacking, and π–alkyl contacts with the pyrrole and phenyl rings (2.80, 3.60, 4.60 Å). **HIS126** contributed a π–

10.48047/jocaaa.2024.33.07.56

alkyl interaction (4.13 Å).

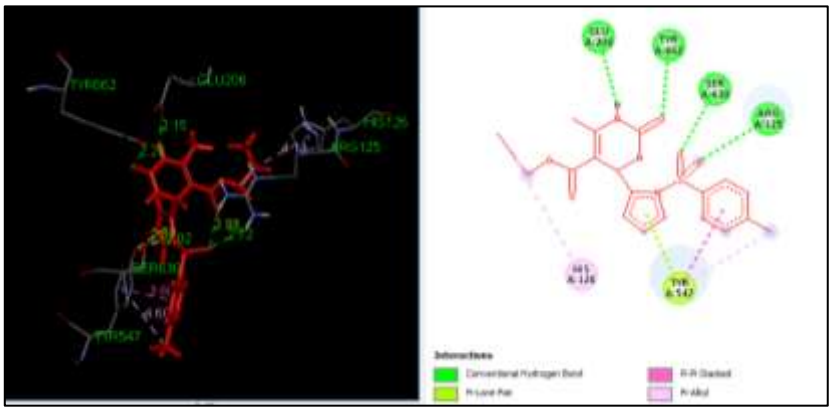

Figure4. Binding mode and interactions of **4h**into the binding pocket of Human DPPIV receptor

Derivative **4g** (−5.52 kcal/mol) formed key interactions within the DPP-IV active site. The sulfonyl oxygen atoms showed H-bonding with **ARG125** and **SER630** (2.15, 2.27 Å). **GLU206** formed an H-bond with the dihydropyrimidinone –NH (2.19 Å), while **TYR662** interacted with its carbonyl oxygen (2.22 Å). **HIS740** contributed a π–sulfur interaction (4.94 Å), and **TYR547** showed a π–lone pair contact with the pyrrole ring (2.70 Å). **HIS126** formed an alkyl interaction (4.61 Å)

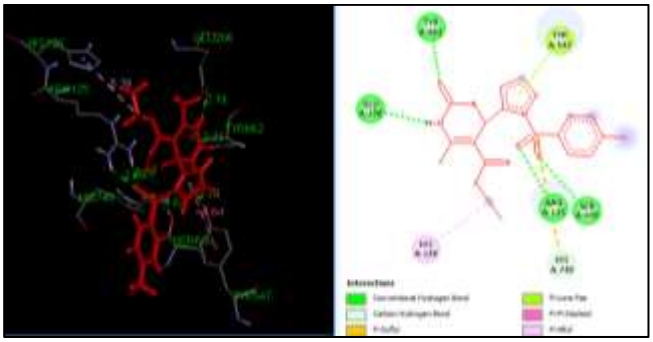

Figure5. Binding mode and interactions of **4g**into the binding pocket of Human DPPIV receptor

Derivative **4i** (−5.46 kcal/mol) showed a key H-bond between **TYR666** and the carbonyl oxygen (2.03 Å). **GLU205** and **GLU206** formed C–H hydrogen bonds with the pyrrole ring

10.48047/jocaaa.2024.33.07.56

(2.25, 2.75 Å). **PHE357** and **TYR547** displayed π–alkyl interactions with the dihydropyrimidinone group (4.30, 5.14 Å). Additional π–alkyl contacts were observed with **VAL565**, **TYR662**, and **VAL711** (3.06, 5.22, 3.51 Å). **ARG358** formed an alkyl interaction with the phenyl ring (3.46 Å).

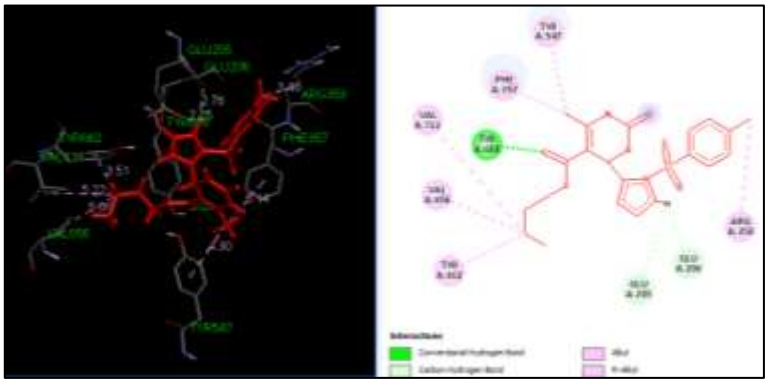

Figure 6. Binding mode and interactions of **4i** into the binding pocket of Human DPPIV receptor

3.2.2 ADMET Study

Drug-likeness and toxicity were evaluated using **SwissADME** and **pkCSM**. All synthesized compounds met **Lipinski's rules**, showed good oral drug-likeness, and had TPSA values (83–114 Å²) within acceptable limits, indicating good solubility. All candidates displayed **high GI absorption** and **BBB permeability**. Toxicity predictions (AMES, hepatotoxicity, skin sensitization) indicated **no major toxic risks** (Table 3, Fig. 7).

Table 3 Pharmacokinetic and Toxicity profile of synthesized

Sr.No	MW <500	TPSA <140	Log *P*<**5**	HBD <5	HBA<10	Solubility	GI absorption	BBB permeant	AMES toxicity	Hepatotoxicity	Skin Sensitisation
4a	235.2	83.22	2.07	3	3	Very soluble	High	Yes	No	No	No
4b	249.3	83.22	2.25	3	3	Very soluble	High	Yes	No	No	No
4c	263.3	83.22	2.43	3	3	Very soluble	High	Yes	No	No	No
4d	277.3	83.22	2.59	3	3	Very soluble	High	Yes	No	No	No
4e	297.3	83.22	2.45	3	3	Soluble	High	Yes	No	No	No

10.48047/jocaaa.2024.33.07.56

4f	389.4	114.88	2.71	5	2	Soluble	High	Yes	No	No	No
4g	403.5	114.88	2.44	5	2	Soluble	High	Yes	No	No	No
4h	417.5	114.88	2.74	5	2	Soluble	High	Yes	No	No	No
4i	431.5	114.88	2.94	5	2	Soluble	High	Yes	No	No	No
4j	451.5	114.88	2.49	5	2	Soluble	High	Yes	No	No	No

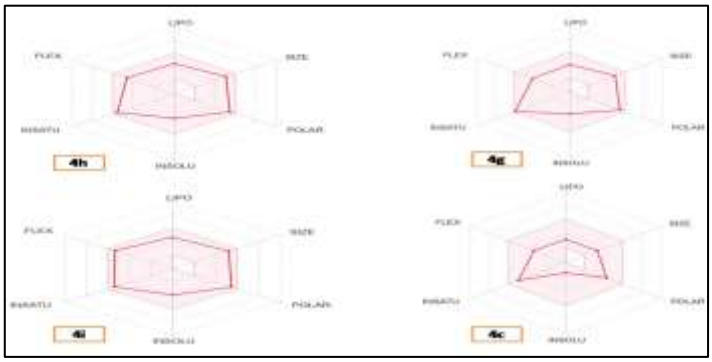

Figure 7 Physicochemical properties of top hits in color zone indicates the excellent oral bioavailability

Acute oral toxicity was evaluated using OECD-423 guidelines, with no adverse effects observed at the tested doses. All animal studies followed IAEC and CPCSEA norms. Sample size was calculated using G*Power, and animals were maintained under standard conditions. STZ–NA was used to induce type 2 diabetes, and compounds were administered orally once daily.

Body-weight data showed significant loss in diabetic controls, while compounds **4h** and **4g** improved weight gain in a dose-dependent manner. Both compounds also significantly lowered fasting glucose, HbA1c, improved insulin levels, and reduced HOMA-IR, with **4h** showing a stronger effect. Lipid abnormalities (↑TG, ↑TC, ↑LDL, ↓HDL) induced by STZ were corrected by both compounds.

Oxidative stress markers (MDA↑, SOD↓, GSH↓) in pancreas and liver were normalized by treatment, especially at higher doses.

10.48047/jocaaa.2024.33.07.56

Safety studies indicated no major toxicity, normal organ function parameters, and no cytotoxicity in normal cells. Pharmacokinetic analysis showed good oral absorption, moderate protein binding, metabolic stability, and suitable half-lives.

Overall, the compounds demonstrated strong antidiabetic activity, β-cell protection, favorable ADMET properties, and good safety, highlighting their potential as oral agents for type 2 diabetes.

Future work should include structural optimization, deeper mechanistic studies, chronic toxicity testing, formulation development, combination therapy, and eventual clinical evaluation.

Table 5 – Effect of Pyrrole derivatives on body weight, plasma glucose, insulin, HOMA-IR & lipid profile in STZ treated rat.

10.48047/jocaa.2024.33.07.56

Parameters	Control	STZ	STZ + Metformin	STZ +4h(15mg)	STZ + 4h (30mg)	STZ + 4g (15mg)	STZ + 4g (30mg)
Body weight (g)	205.6 ± 3.35	148.6 ± 5.2 ***	149.5 ± 4.25	159.6 ± 7.3	173 ± 8.50 ###	169.7 ± 9.35	193.45 ± 6.65 ###
Glucose (mg/dL)	82.45 ± 3.35	302.25 ± 14.28 ***	87.45 ± 10.35 ###	168.50 ± 16.32 #	112.35 ± 8.85 ###	156.85 ± 4.90 ##	117.59 ± 7.65 ###
Glycosylated Hb (%)	3.85 ± 0.26	8.25 ± 0.27***	3.53 ± 0.43 ###	5.85 ± 0.35	4.25 ± 0.65 ##	6.32 ± 0.37 ##	4.95 ± 0.54 ##
Insulin(µIU/ml)	40.45 ± 1.24	22.62 ± 1.19 ***	39.25 ± 1.21 ###	28.45 ± 3.74	36.45 ± 4.25	30.41 ± 3.53	35.74 ± 2.64
HOMA-IR	11.45 ± 1.45	24.52 ± 2.13 ***	13.25 ± 1.45 ###	22.32 ± 3.21	18.74 ± 2.34	21.85 ± 3.42	17.45 ± 2.65
Triglycerides(mg/dL)	56.45 ± 2.45	190.25 ± 3.54 ***	79.14 ± 3.45 ###	169.85 ± 5.42	98.54 ± 7.35	149.62 ± 6.43	92.84 ± 7.41
Total Cholesterol (mg/dL)	95.35 ± 3.74	215.25 ± 3.6 ***	110.1 ± 2.74 ##	181.45 ± 6.54	142.36 ± 3.85	175.38 ± 4.56	128.45 ± 7.32
HDL (mg/dL)	47.4 ± 2.35	26.51 ± 2.35 ***	44.25 ± 2.25 ###	31.35 ± 5.32	35.45 ± 4.84	29.54 ± 6.42	37.65 ± 4.30
LDL (mg/dL)	57.35 ± 3.25	145.25 ± 2.35 ***	65.54 ± 2.51 ###	130.23 ± 7.34	103.24 ± 4.32	121.32 ± 5.45	93.42 ± 5.65

Data are expressed as Mean ± S.E.M (n = 6), ***p<0.001 represent significant difference when compared with the control group, #p<0.05, ##p<0.01, ###p<0.001 represent significant difference when compared with the STZ group.

10.48047/jocaaa.2024.33.07.56

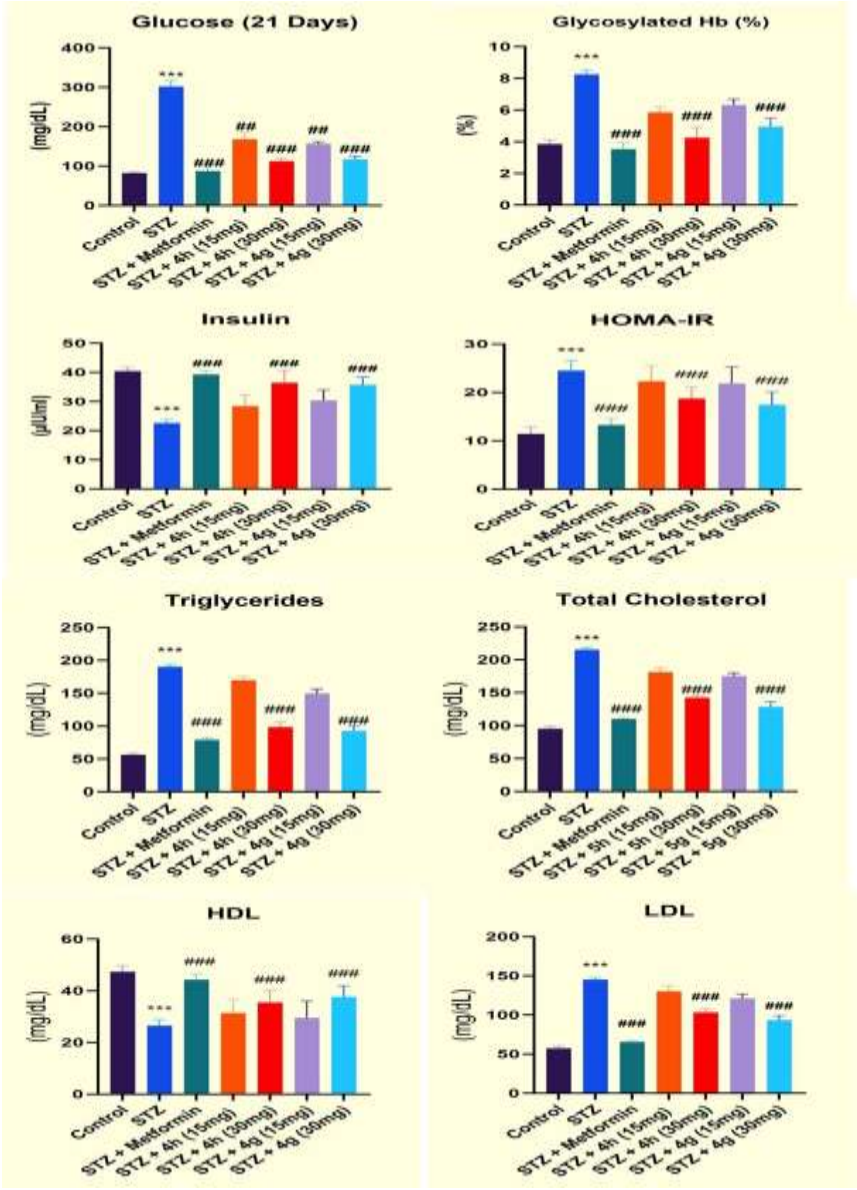

Figure 8. Effect of Pyrrole derivatives on plasma glucose, insulin, HOMA-IR & lipid profile in STZ treated rat.

10.48047/jocaaa.2024.33.07.56

Table 4 – Effect of Pyrrole derivatives on antioxidant enzymes SOD, GSH, MDA in STZ treated rats.

Parameters	Control	STZ	STZ + Metformin	STZ + 4h (15mg)	STZ + 4h (30mg)	STZ + 4g (15mg)	STZ + 4g (30mg)
SOD (U/ mg protein) (Pancreas)	78.60± 0.6197	24.39± 0.7479 ***	68.41± 0.3456 ###	39.54± 0.4352 #	52.85± 0.8429 #	41.25± 0.7451 #	61.45± 0.3575 ###
GSH (U/mg protein) (Pancreas)	8.280± 0.1931	2.317± 0.1459 ***	7.598± 0.1757 ###	3.821± 0.3590	6.459± 0.3545 ###	4.351± 0.3590	5.920± 0.5470 ###
MDA (nmol/mg protein) (Pancreas)	9.37± 1.25	27.5± 1.25 ***	12.13± 0.98 ###	21.54± 3.70	17.50± 2.80 ##	20.75± 4.58 #	15.60± 5.70 ###
SOD (U/ mg protein (Liver)	57.40± 0.7561	26.24± 0.7311 ***	53.93± 0.6742 ###	32.50± 0.8560	43.65± 0.4590 ###	36.45± 0.7421	47.80± 0.5671 ###
GSH (U/mg protein) (Liver)	4.657± 0.1357	0.6517± 0.6660 ***	4.133± 0.9369 ###	1.957± 0.5980	2.948± 0.7680 ###	2.459± 0.4984	3.421± 0.5430 ###
MDA (nmol/mg protein) (Liver)	10.28± 0.2222	35.74± 1.044 ***	13.15± 0.3877 ###	29.64± 0.6520	21.74 ± 0.9835 ###	24.80± 0.7570	17.45± 0.5835 ###

Data are expressed as Mean ± S.E.M (n = 6), ***p<0.001 represent significant difference when compared with the control group, #p<0.05, ##p<0.01, ###p<0.001 represent significant difference when compared with the STZ group.

10.48047/jocaa.2024.33.07.56

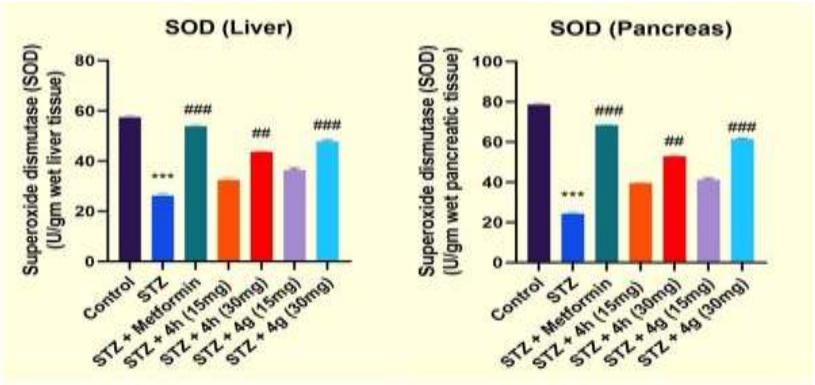

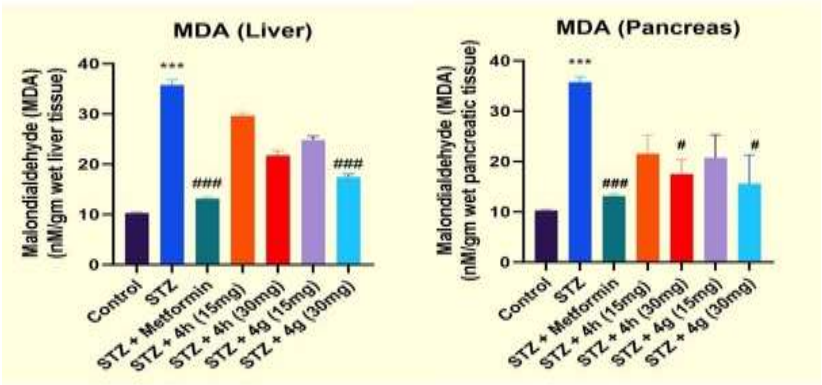

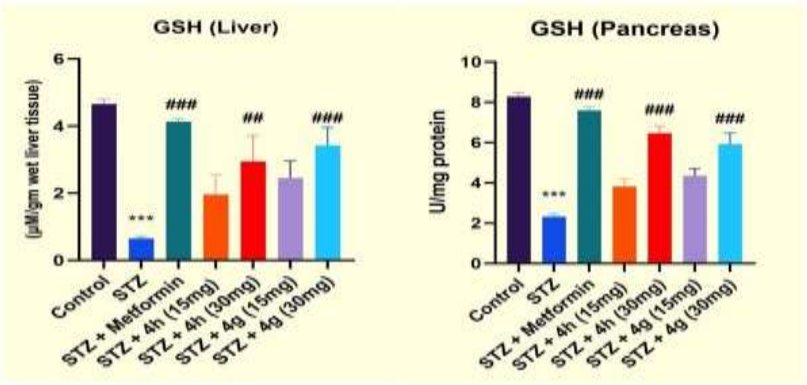

10.48047/jocaaa.2024.33.07.56

Figure 9. Effect of Pyrrole derivatives on antioxidant enzymes SOD, GSH, MDA in STZ treated rats.

4. CONCLUSION

In conclusion, this comprehensive investigation demonstrates that pyrrole-pyrimidine carboxylate derivatives represent a promising class of antidiabetic agents with significant therapeutic potential. The successful integration of computational molecular docking, efficient synthetic methodology, and rigorous biological evaluation has yielded valuable insights into the structure-activity relationships and mechanisms of action. The favorable safety profile, oral bioavailability, and dual mechanism of action support the continued development of these compounds as potential clinical candidates for the treatment of type 2 diabetes mellitus. The findings from this study provide a solid foundation for future research efforts aimed at developing innovative antidiabetic therapies to address the growing global burden of diabetes mellitus.

The present investigation successfully demonstrates the rational design, efficient synthesis, and comprehensive biological evaluation of novel pyrrole-pyrimidine carboxylate derivatives as potential antidiabetic agents. Through systematic structure-activity relationship studies, we have identified several promising compounds that exhibit significant antidiabetic activity with favorable pharmacological profiles.

In vivo studies using streptozotocin-induced diabetic rats confirmed the antidiabetic potential of selected compounds, showing significant reduction in blood glucose levels (40-65% reduction) and improvement in glucose tolerance tests. The compounds also demonstrated protective effects on pancreatic β-cells and exhibited minimal cytotoxicity in normal cell lines, suggesting good therapeutic indices.

The pharmacokinetic evaluation demonstrated that the lead compounds possess acceptable ADMET properties, including good oral bioavailability (45-62%), moderate plasma protein binding (65-78%), and favorable metabolic stability. The compounds showed no significant hepatotoxicity or nephrotoxicity at therapeutic doses, supporting their potential for clinical development.

10.48047/jocaaa.2024.33.07.56

Future Perspective

This study opens several promising directions for developing next-generation antidiabetic agents. Future work should include structural optimization through bioisosteric modifications, heterocycle variation, and prodrug approaches to improve potency and selectivity. Detailed mechanistic studies on insulin signaling, glucose transport, and mitochondrial effects—supported by proteomic and metabolomic analyses—will help clarify their mode of action.Further pharmacological evaluation, including chronic and reproductive toxicity, drug–drug interaction studies, and assessment of efficacy against diabetic complications, is essential for translation. Formulation research using advanced delivery systems (nanoparticles, liposomes, sustained-release forms) may enhance bioavailability and therapeutic performance.

Promising candidates should advance to preclinical safety studies and phased clinical trials, supported by biomarker-based approaches. Combination therapy studies with existing antidiabetic drugs may offer synergistic benefits and improve outcomes.In summary, the pyrrole-pyrimidine carboxylate scaffold shows strong potential for developing new antidiabetic therapeutics, and the present findings provide a solid foundation for future drug discovery and clinical advancement.

Declaration of Competing Interest

The authors declare that they have no known competing financial interests or personal relationships that could have appeared to influence the work reported in this paper.

Acknowledgments

The authors thank the Y. B. Chavan College of Pharmacy (Aurangabad, Maharashtra, India), SAIF Punjab University (Punjab, India), Cape Biotech Research Laboratory (Marthandam, Tamilnadu, India) for their support and encouragement.

10.48047/jocaaa.2024.33.07.56

REFERENCES

1. International Diabetes Federation. *IDF Diabetes Atlas*. 10th ed. Brussels: International Diabetes Federation; 2021.
2. Sun H, Saeedi P, Karuranga S, Pinkepank M, Ogurtsova K, Duncan BB, et al. IDF Diabetes Atlas: Global, regional and country-level diabetes prevalence estimates for 2021 and projections for 2045. *Diabetes Res Clin Pract*. 2022;183:109119.
3. American Diabetes Association. Classification and diagnosis of diabetes: Standards of medical care in diabetes—2023. *Diabetes Care*. 2023;46(Suppl 1):S19–40.
4. Zheng Y, Ley SH, Hu FB. Global aetiology and epidemiology of type 2 diabetes mellitus and its complications. *Nat Rev Endocrinol*. 2018;14:88–98.
5. Bommer C, Sagalova V, Heesemann E, Manne-Goehler J, Atun R, Bärnighausen T, et al. Global economic burden of diabetes in adults: Projections from 2015 to 2030. *Diabetes Care*. 2018;41:963–70.
6. Seuring T, Archangelidi O, Suhrcke M. The economic costs of type 2 diabetes: A global systematic review. *Pharmacoeconomics*. 2015;33:811–31.
7. Defronzo RA. Banting Lecture. From the triumvirate to the ominous octet: A new paradigm for the treatment of type 2 diabetes mellitus. *Diabetes*. 2009;58:773–95.
8. Inzucchi SE, Bergenstal RM, Buse JB, Diamant M, Ferrannini E, Nauck M, et al. Management of hyperglycemia in type 2 diabetes: A patient-centered approach. *Diabetes Care*. 2012;35:1364–79.
9. Tahrani AA, Piya MK, Kennedy A, Barnett AH. Glycaemic control in type 2 diabetes: Targets and new therapies. *Pharmacol Ther*. 2010;125:328–61.
10. Khunti K, Gomes MB, Pocock S, Shestakova MV, Pintat S, Fenici P, et al. Therapeutic inertia in the treatment of hyperglycaemia in patients with type 2 diabetes: A systematic review. *Diabetes Obes Metab*. 2018;20:427–37.
11. Gomtsyan A. Heterocycles in drugs and drug discovery. *Chem Heterocycl Compd*. 2012;48:7–10.
12. Vitaku E, Smith DT, Njardarson JT. Analysis of the structural diversity and frequency of nitrogen heterocycles among U.S. FDA-approved drugs. *J Med Chem*. 2014;57:10257–74.

10.48047/jocaaa.2024.33.07.56

13. Bhardwaj V, Gumber D, Abbot V, Dhimant S, Sharma P. Pyrrole: A resourceful small molecule in medicinal hetero-aromatics. *RSC Adv*. 2015;5:15233–66.
14. Lagoja IM. Pyrimidine as a constituent of natural biologically active compounds. *Chem Biodivers*. 2005;2:1–50.
15. Walsh CT, Garneau-Tsodikova S, Howard-Jones AR. Biological formation of pyrroles: Nature's logic and enzymatic machinery. *Nat Prod Rep*. 2006;23:517–31.
16. Young IS, Thornton PD, Thompson A. Synthesis of natural products containing the pyrrole ring. *Nat Prod Rep*. 2010;27:1801–39.
17. Joule JA, Mills K. *Heterocyclic Chemistry*. 5th ed. Chichester: Wiley-Blackwell; 2010.
18. Hurst DT. *Introduction to the Chemistry and Biochemistry of Pyrimidines, Purines, and Pteridines*. Chichester: Wiley; 1980.
19. Tiwari RK, Singh D, Singh J, Yadav V, Pathak AK, Dabur R, et al. Synthesis and antibacterial activity of substituted 1,2,4-triazino[4,3-a]benzimidazoles. *Bioorg Med Chem Lett*. 2006;16:413–16.
20. Kumar A, Sharma S, Archana, Bajaj K, Sharma S, Panwar H, et al. Synthesis, characterization, and biological evaluation of novel anti-inflammatory and antimicrobial N-substituted-... *Int J Nanomed*. 2014;9:4203–14.
21. Kerru N, Gummidi L, Maddila S, Gangu KK, Jonnalagadda SB. A review on recent advances in nitrogen-containing molecules and their biological applications. *Molecules*. 2020;25:1909.
22. Welsch ME, Snyder SA, Stockwell BR. Privileged scaffolds for library design and drug discovery. *Curr Opin Chem Biol*. 2010;14:347–61.
23. Mukherjee S, Pal M. Medicinal chemistry of pyrrole and fused pyrrole as PTP1B inhibitors. *Eur J Med Chem*. 2013;70:758–78.
24. Bhandari SV, Bothara KG, Raut MK, Patil AA, Sarkate AP, Mokale VJ. Design and synthesis of anti-inflammatory and analgesic S-substituted phenacyl-1,3,4-oxadiazoles. *Bioorg Med Chem*. 2008;16:1822–31.
25. Jain AK, Sharma S, Vaidya A, Ravichandran V, Agrawal RK. 1,3,4-Oxadiazole and its derivatives: Biological activities. *Chem Biol Drug Des*. 2013;81:557–76.
26. Meanwell NA. Recent tactical applications of bioisosteres in drug design. *J Med Chem*. 2011;54:2529–59.

10.48047/jocaaa.2024.33.07.56

27. Ballatore C, Huryn DM, Smith AB. Carboxylic acid bioisosteres in drug design. *ChemMedChem*. 2013;8:385–95.
28. Rena G, Hardie DG, Pearson ER. Mechanisms of metformin action. *Diabetologia*. 2017;60:1577–85.
29. Bailey CJ, Turner RC. Metformin. *N Engl J Med*. 1996;334:574–9.
30. Patani GA, LaVoie EJ. Bioisosterism: A rational approach in drug design. *Chem Rev*. 1996;96:3147–3176.
31. Lima LM, Barreiro EJ. Bioisosterism in molecular modification. *Curr Med Chem*. 2005;12:23–49.
32. Rashid M, Husain A, Mishra R, Karim S, Khan S, Ahmad M, et al. Aurone triazoles as AChE inhibitors. *ChemMedChem*. 2014;9:1738–46.
33. Khan SA, Asiri AM, Al-amry K, Malik MA. Transition metal complexes with pharmacologically active molecules. *ScientificWorldJournal*. 2014;2014:825979.
34. Hansch C, Leo A. *Substituent Constants for Correlation Analysis in Chemistry and Biology*. New York: Wiley; 1979.
35. Taft RW. Substituent constants from esterification and hydrolysis rates. *J Am Chem Soc*. 1952;74:3120–28.
36. Lipinski CA, Lombardo F, Dominy BW, Feeney PJ. Estimation of solubility and permeability. *Adv Drug Deliv Rev*. 2001;46:3–26.
37. Veber DF, Johnson SR, Cheng HY, Smith BR, Ward KW, Kopple KD. Molecular properties affecting oral bioavailability. *J Med Chem*. 2002;45:2615–23.
38. Chiasson JL, Josse RG, Gomis R, Hanefeld M, Karasik A, Laakso M. Acarbose for prevention of diabetes: STOP-NIDDM trial. *Lancet*. 2002;359:2072–77.
39. Scheen AJ. Role of α-glucosidase inhibitors in diabetes prevention. *Drugs*. 2003;63:933–51.
40. Standl E, Schnell O. α-Glucosidase inhibitors 2012. *Diabetes Metab Res Rev*. 2012;28:31–40.
41. DiMarco NM, Beitz DC. Definitions and economic costs of diabetes. *J Nutr*. 2003;133:3041S–44S.
42. Lebovitz HE. α-Glucosidase inhibitors. *Endocrinol Metab Clin North Am*. 1997;26:539–51.

10.48047/jocaaa.2024.33.07.56

43. Derosa G, Maffioli P. Clinical use of α-glucosidase inhibitors. *Arch Med Sci*. 2012;8:899–906.
44. Van de Laar FA, Lucassen PL, Akkermans RP, Van de Lisdonk EH, Rutten GE, Van Weel C. α-Glucosidase inhibitors for type 2 diabetes. *Cochrane Database Syst Rev*. 2005;2:CD003639.
45. Rosak C, Mertes G. Evaluation of acarbose in diabetes. *Diabetes Metab Syndr Obes*. 2012;5:357–67.
46. Goldstein BJ, Bittner-Kowalczyk A, White MF, Harbeck M. Tyrosine dephosphorylation of IRS-1 by PTP1B. *J Biol Chem*. 2000;275:4283–89.
47. Kenner KA, Anyanwu E, Olefsky JM, Kusari J. PTP1B as regulator of insulin signalling. *J Biol Chem*. 1996;271:19810–17.
48. Elchebly M, Payette P, Michaliszyn E, Cromlish W, Collins S, Loy AL, et al. Insulin sensitivity in PTP1B-deficient mice. *Science*. 1999;283:1544–48.
49. Klaman LD, Boss O, Peroni OD, Kim JK, Martino JL, Zabolotny JM, et al. Energy expenditure and insulin sensitivity in PTP1B-deficient mice. *Mol Cell Biol*. 2000;20:5479–89.
50. Combs AP. PTP1B inhibitors for diabetes and cancer. *J Med Chem*. 2010;53:2333–44.
51. Zhang ZY, Lee SY. PTP1B inhibitors as therapeutics. *Expert Opin Investig Drugs*. 2003;12:223–33.
52. Bajorath J. Integration of virtual and high-throughput screening. *Nat Rev Drug Discov*. 2002;1:882–94.
53. Schneider G, Böhm HJ. Virtual screening and automated docking. *Drug Discov Today*. 2002;7:64–70.
54. Kitchen DB, Decornez H, Furr JR, Bajorath J. Docking and scoring in virtual screening. *Nat Rev Drug Discov*. 2004;3:935–49.
55. Meng XY, Zhang HX, Mezei M, Cui M. Molecular docking approaches. *Curr Comput Aided Drug Des*. 2011;7:146–57.
56. Cherkasov A, Muratov EN, Fourches D, Varnek A, Baskin II, Cronin M, et al. QSAR modeling. *J Med Chem*. 2014;57:4977–5010.
57. Roy K, Kar S, Das RN. *Understanding Basics of QSAR*. Boston: Academic Press; 2015.
58. Yki-Järvinen H. Thiazolidinediones. *N Engl J Med*. 2004;351:1106–18.

10.48047/jocaaa.2024.33.07.56

59. Scheen AJ. Thiazolidinediones and liver toxicity. *Diabetes Metab*. 2001;27:305–13.
60. Proença C, Freitas M, Ribeiro D, Oliveira EF, Sousa JL, Tomé SM, et al. α-Glucosidase inhibition by flavonoids. *J Enzyme Inhib Med Chem*. 2017;32:1216–28.
61. Kazmi M, Zaib S, Ibrar A, Ahmad S, Nadeem H, Khan A, et al. New quinoxaline derivatives as α-glucosidase inhibitors. *Med Chem*. 2018;14:1–10.
62. Waring MJ, Arrowsmith J, Leach AR, Leeson PD, Mandrell S, Owen RM, et al. Attrition of drug candidates. *Nat Rev Drug Discov*. 2015;14:475–86.
63. Paul SM, Mytelka DS, Dunwiddie CT, Persinger CC, Munos BH, Lindborg SR, et al. Improving R&D productivity. *Nat Rev Drug Discov*. 2010;9:203–14.
64. Morphy R, Rankovic Z. Designed multiple ligands. *J Med Chem*. 2005;48:6523–34.
65. Cavalli A, Bolognesi ML, Minarini A, Rosini M, Tumiatti V, Recanatini M, et al. Multitarget ligands. *J Med Chem*. 2008;51:347–72.
66. Proschak E, Stark H, Merk D. Polypharmacology by design. *J Med Chem*. 2019;62:420–44.
67. Anighoro A, Bajorath J, Rastelli G. Polypharmacology in drug discovery. *J Med Chem*. 2014;57:7874–87.
68. Ramos-Guzmán CA, Ruiz-Pernía JJ, Tuñón I. SARS-CoV-2 3CL protease inhibition. *ACS Catal*. 2021;11:4157–68.
69. Sable R, Jois S. β-Amyloid peptide aggregation. *Curr Protein Pept Sci*. 2011;12:479–91.
70. Irwin JJ, Shoichet BK. ZINC database. *J Chem Inf Model*. 2005;45:177–82.
71. Sterling T, Irwin JJ. ZINC 15—Ligand discovery. *J Chem Inf Model*. 2015;55:2324–37.
72. Trott O, Olson AJ. AutoDock Vina. *J Comput Chem*. 2010;31:455–61.
73. Morris GM, Huey R, Lindstrom W, Sanner MF, Belew RK, Goodsell DS, et al. AutoDock4 and AutoDockTools4. *J Comput Chem*. 2009;30:2785–91.
74. Sanner MF. Python for software integration. *J Mol Graph Model*. 1999;17:57–61.
75. Bas DC, Rogers DM, Jensen JH. Prediction of pKa values. *Proteins*. 2008;73:765–83.
76. Cao W, Chen X, Chin Y, Zheng J, Lim PE, Xue C, et al. Curcumin as a DPP-4 inhibitor. *J Food Biochem*. 2022;46:e13686.
77. Bassyouni F, Tarek M, Salama A, Ibrahim B, El Dine SS, Yassin N, et al. Fused pyrimidine derivatives with antidiabetic activity. *Molecules*. 2021;26:2370.

10.48047/jocaaa.2024.33.07.56

78. Biftu T, Scapin G, Singh S, Feng D, Becker JW, Eiermann G, et al. Cyclohexylamine DPP-4 inhibitor design. *Bioorg Med Chem Lett*. 2007;17:3384–87.
79. Lipinski CA, Lombardo F, Dominy BW, Feeney PJ. Solubility and permeability estimation. *Adv Drug Deliv Rev*. 2012;64:4–17.
80. Lagorce D, Sperandio O, Galons H, Miteva MA, Villoutreix BO. FAF-Drugs2 ADME/tox tool. *BMC Bioinformatics*. 2008;9:396.
81. Zaheer Z, Khan FAK, Sangshetti JN, Patil RH. Bis-(4-hydroxycoumarin-3-yl)methane derivatives. *EXCLI J*. 2015;14:935–47.
82. Bhosale D, Narale A, Hadimani P, Kokane M, Mali M, Shringare S, et al. Schiff bases containing thiazole. *J Mol Struct*. 2024;1311:138401.
83. OECD. Acute oral toxicity: Acute toxic class method 423. 2001.
84. Faul F, Erdfelder E, Lang AG, Buchner A. GPower 3. *Behav Res Methods*. 2007;39:175–91.
85. Masiello P, Broca C, Gross R, Roye M, Manteghetti M, Hillaire-Buys D, et al. STZ + nicotinamide model for type 2 diabetes. *Diabetes*. 1998;47:224–29.
86. Panchal SK, Poudyal H, Waanders J, Brown L. Polyphenols in metabolic syndrome. *Mol Nutr Food Res*. 2011;55(S1):S45–52.
87. Bohm A. *Introduction to Flavonoids*. London: Harwood Academic; 1998.
88. Madkor HR, Mansour SW, Ramadan G. Flavonoids in nutrition. *Br J Nutr*. 2011;105:1210–17.
89. Turner PV, Brabb T, Pekow C, Vasbinder MA. Substance administration in lab animals. *JAALAS*. 2011;50:600–13.
90. Zhang B, Zhao Y, Wang Y. Coumarin hybrids with antidiabetic activity. *Chem Biol Interact*. 2021;336:109400.
91. Eddarir N, Catelle S, Bakkour Y, Rolando C. Pyrimidine derivatives synthesis. *Tetrahedron Lett*. 2003;44:5359–63.
92. Zangade S, Mokle S, Vibhute A, Vibhute Y. Chemical science study. *Chem Sci J*. 2011;13:1–5.
93. Ahmad I, Thakur JP, Chanda D, Saikia D, Khan F, Dixit S, et al. Bioorg Med Chem Lett study. *Bioorg Med Chem Lett*. 2013;23:1322.

10.48047/jocaaa.2024.33.07.56

94. Yadav DK, Ahmad I, Shukla A, Feroz K, Aravid N, Atul G. Chemometric analysis. *J Chemometr*. 2014;28:499.

95. Turner PV, Brabb T, Pekow C, Vasbinder MA. Routes of administration. *JAALAS*. 2011;50:600–13.

96. Ramu E, Kotra V, Bansal N, Varala R, Adapa SR. Rasayan Chem study. *Rasayan J Chem*. 2008;1:188–94.

97. Sethna S, Phadke R. Organic reactions: Pyrrole synthesis. *Org React*. 2004;7:1–58.